Frontiers of Physics
https://doi.org/10.1007/s11467-021-1128-z
Front. Phys.
17(3), 31502 (2022)

RESEARCH ARTICLE

Nonadiabatic geometric quantum computation protected by dynamical decoupling via the *XXZ* Hamiltonian

X. Wu, P. Z. Zhao†

Department of Physics, Shandong University, Jinan 250100, China
Corresponding author. E-mail: †*pzzhao@email.sdu.edu.cn*
Received August 23, 2021; accepted October 26, 2021

Nonadiabatic geometric quantum computation protected by dynamical decoupling combines the robustness of nonadiabatic geometric gates and the decoherence-resilience feature of dynamical decoupling. Solid-state systems provide an appealing candidate for the realization of nonadiabatic geometric quantum computation protected dynamical decoupling since the solid-state qubits are easily embedded in electronic circuits and scaled up to large registers. In this paper, we put forward a scheme of nonadiabatic geometric quantum computation protected by dynamical decoupling via the *XXZ* Hamiltonian, which not only combines the merits of nonadiabatic geometric gates and dynamical decoupling but also can be realized in a number of solid-state systems, such as superconducting circuits and quantum dots.

Keywords nonadiabatic geometric quantum computation, dynamical decoupling, *XXZ* Hamiltonian

1 Introduction

Quantum computation is founded on quantum-mechanical principles and provides an efficient solution to certain problems, such as factoring large integers [1] and searching unsorted data [2]. To implement practical quantum computation, a universal set of high-fidelity quantum gates, including arbitrary one-qubit gates and a nontrivial two-qubit gate [3], needs to be realized. However, the control errors accumulated in the operation processing inevitably affect quantum gates and thus result in a decreased fidelity of quantum gates. To overcome this problem, quantum computation based on geometric phases was proposed. Geometric gates depend only on evolution paths but not on evolution details, making them robust against control errors.

Geometric quantum computation was initially put forward based on adiabatic Abelian geometric phases [4] or adiabatic non-Abelian geometric phases [5], which is referred to as adiabatic geometric quantum computation [6] or adiabatic holonomic quantum computation [7, 8]. However, acquiring adiabatic geometric phases needs the quantum system to undergo long-run-time evolution [9–11]. To avoid this problem, nonadiabatic geometric quantum computation [12, 13] based on nonadiabatic Abelian geometric phases [14] was proposed, and further nonadiabatic holonomic quantum computation [15, 16] based on nonadiabatic non-Abelian geometric phases [17] was put forward. Considering that nonadiabatic non-Abelian geometric phases are generated by the cyclic evolution and parallel transport of a state subspace in the Hilbert space, the realization of nonadiabatic holonomic gates needs auxiliary states in addition to the computational states. Different from nonadiabatic holonomic gates, nonadiabatic geometric gates, which are based on nonadiabatic Abelian geometric phases generated by the cyclic evolution of quantum states with the removal of dynamical phases, can be realized with the computational states themselves. Up to now, nonadiabatic geometric quantum computation has been well developed in both theories [18–44] and experiments [45–48].

For the achievement of high-fidelity quantum gates, the decoherence caused by the interaction between the quantum system and its environment is another main obstacle. Dynamical decoupling is an active quantum control technique to filter out the undesired effects from the environment [49]. To further improve the fidelity of quantum gates, it is a promising strategy to protect nonadiabatic geometric gates by using dynamical decoupling [31–33]. Solid-state systems provide an appealing candidate for the realization of nonadiabatic geometric quantum computation protected dynamical decoupling since the solid-state qubits are easily embedded in electronic circuits and scaled up to large registers. As a solid-state system, the superconducting circuit, being one of the most promising platforms for the realization of quantum computation, has been utilized to experimentally realize nonadiabatic geo-

* This article can also be found at http://journal.hep.com.cn/fop/EN/10.1007/s11467-021-1128-z.

metric gates [47, 48].

In this paper, we put forward a scheme of nonadiabatic geometric quantum computation protected by dynamical decoupling via the XXZ Hamiltonian. This Hamiltonian can be realized in many physical systems [50–67], including but not limited to a number of solid-state systems, such as superconducting circuits [62–64] and quantum dots [65–67]. We further demonstrated that our scheme allows one to realize not only the one-qubit gates about a rotation axis in the x–y plane but also the one-qubit gates about a rotation axis in the y–z plane or x–z plane, indicating the flexibility of our scheme for the realization of universal gates.

2 Physical model

The quantum system in our scheme is comprised of N physical qubits governed by the XXZ Hamiltonian

$$H = \sum_{k<l} (J_{kl}^{xy} R_{kl}^{xy} + J_{kl}^{z} R_{kl}^{z}) \tag{1}$$

with $R_{kl}^{xy} = (\sigma_k^x \sigma_l^x + \sigma_k^y \sigma_l^y)/2$ and $R_{kl}^{z} = \sigma_k^z \sigma_l^z$. Here, J_{kl}^{xy} and J_{kl}^{z} are coupling parameters, and σ_μ^ν denotes the Pauli ν operator acting on the μth physical qubit. This Hamiltonian can be realized in a number of solid-state systems, such as superconducting circuits and quantum dots. In superconducting circuits, the former can be implemented by coupling two superconducting charge qubits with a superconducting quantum interference device and the latter can be implemented by coupling two superconducting charge qubits with a variable electrostatic transformer [62–64]. In quantum dots, it describes the hyperfine dipole–dipole coupling between nuclear spins and the spin of a hole [65–67]. In the following, we take the superconducting circuits as an example to specifically demonstrate how to realize the above Hamiltonian.

We consider a superconducting charge qubit consisting of a superconducting island (Cooper-pair box), which is coupled to a ring by two symmetric Josephson junctions characterized by coupling energy E_J and capacitance C_J [62]. Here, the Josephson coupling energy can be tuned by introducing an external magnetic flux Φ. A control gate voltage V_g is coupled to the system via a gate capacitor C_g. The schematic diagram of the superconducting charge qubit is shown in Fig. 1(a). We choose a material in which the superconducting energy gap Δ is large enough, so that the quasiparticle tunneling is suppressed at low temperatures. We further require that the charging energy E_c is much larger than the coupling energy E_J, where $E_c = 2e^2/(2C_J + C_g)$. In this case, only Cooper pairs tunnel coherently in the superconducting junction. Near the charging energy degeneracy point, only two charge states, i.e., the states with Cooper-pairs $n = 0$ and 1, play a dominant role. Then, the system behaves as a two-level

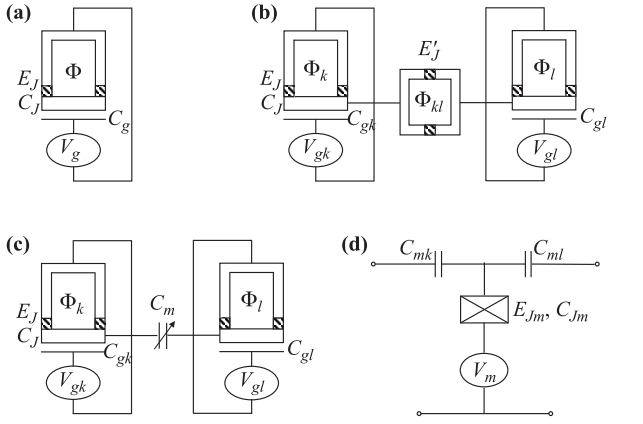

Fig. 1 Schematic diagram for coupled superconducting charge qubits. **(a)** The superconducting charge qubit with tunable effective Josephson coupling. **(b)** The schematic diagram for the realization of the interaction R_{kl}^{xy}. It is implemented by coupling the superconducting charge qubits k and l via a superconducting quantum interference device. **(c)** The schematic diagram for the realization of the interaction R_{kl}^{z}. It is implemented by coupling the superconducting charge qubits k and l via a variable electrostatic transformer C_m. **(d)** Equivalent circuit of the variable electrostatic transformer C_m.

system with the Hilbert space $\{|0\rangle, |1\rangle\}$ and the Hamiltonian reads

$$H = \frac{1}{2} E_c (2n_g - 1)\sigma_z - E_J \cos\left(\pi \frac{\Phi}{\Phi_0}\right) \sigma_x, \tag{2}$$

where $n_g = C_g V_g/(2e)$ is the dimensionless gate charge that can be controlled by the gate voltage V_g and $\Phi_0 = h/(2e)$ is the flux quantum.

To implement the interaction R_{kl}^{xy} in Eq. (1), we need to couple two superconducting charge qubits k and l via a superconducting quantum interference device [63], shown in Fig. 1(b).

If we choose a small junction capacitance of the superconducting quantum interference device, the electrostatic energy between Cooper-pairs boxes k and l can be much smaller than the corresponding Josephson energy. In this case, the effect of electrostatic coupling energy will be ignored and then the interaction Hamiltonian reads

$$H_{kl} = -E'_J \cos\left(\pi \frac{\Phi_{kl}}{\Phi_0}\right) R_{kl}^{xy}, \tag{3}$$

which is the interaction R_{kl}^{xy} in Eq. (1). To implement the interaction R_{kl}^{z} in Eq. (1), we need to couple two superconducting charge qubits to a central island of the transformer by capacitances C_{mk} and C_{ml} [64], shown in Figs. 1(c) and (d). We assume that the structure in Fig. 1(c) is symmetric, i.e., $C_{mk}/C_{\sum_k} = C_{ml}/C_{\sum_l} \equiv c$ with $C_{\sum_k} = C_{mk} + 2C_J + C_{gk}$ and $C_{\sum_l} = C_{ml} + 2C_J + C_{gl}$. In the tight-binding limit, the Hamiltonian related to the transformer can be written as

$$H_{kl} = \nu R_{kl}^{z} + \delta(\sigma_k^z + \sigma_l^z) + \mu. \tag{4}$$

The coupling coefficient ν is given by $\nu = \Delta_m \cos(2\pi q_0)[1-\cos(2\pi c)]/2$, where Δ_m is the characteristic energy gap of the transformer junction and q_0 is the average induced charge reading $q_0 = q_m + c[(n_{gk} - 1/2) + (n_{gl} - 1/2)]$ with $q_m = V_m(C_{mk} + C_{ml})(1 - c)/(2e)$. The coefficient δ of the charging energy shift is given by $\delta = \Delta_m \cos(2\pi q_0)\cos(2\pi c)/2$ and μ is a constant term that can be ignored. If we set $c = 1/4$, the above Hamiltonian yields the interaction R^z_{kl} in Eq. (1). Therefore, the XXZ Hamiltonian can be realized by combining Eqs. (3) and (4), where the single-qubit Hamiltonian has been removed by introducing an off-resonant microwave pulse for the elimination of the first part in Eq. (2) and setting $\Phi = \Phi_0/2$ for the elimination of the second part.

For the quantum system governed by the Hamiltonian in Eq. (1), we consider the following interaction Hamiltonian

$$H_I = \sum_{k,\nu} \sigma^\nu_k \otimes B^\nu_k, \tag{5}$$

where B^ν_k is the environment operator. The undesired effects caused by the above interaction Hamiltonian can be filtered out by using dynamical decoupling [49, 68].Specifically, we apply a periodic sequence with decoupling group $\mathcal{G} = \{g_k\}^{|\mathcal{G}|-1}_{k=0}$ to the quantum system over a period of time T, where $|\mathcal{G}|$ is the order of the group, g_0 is an identity operator, and g_k are unitary operators acting on the quantum system. If each pulse g_k is instantaneous and the period of time T is set to satisfy $T = |\mathcal{G}|\Delta t \to 0$ with Δt being the duration time of pulse intervals, then the interaction Hamiltonian is reduced to $H'_I = (1/|\mathcal{G}|)\sum_{g_k\in\mathcal{G}} g^\dagger_k H_I g_k$. By choosing the decoupling group as $\mathcal{G} = \{\otimes^N_{k=1} I_k, \otimes^N_{k=1}\sigma^x_k, \otimes^N_{k=1}\sigma^y_k, \otimes^N_{k=1}\sigma^z_k\}$, the interaction Hamiltonian will be filtered out. To make the quantum system not only be protected by dynamical decoupling but also complete the desired evolution, we need the Hamiltonian to commute with the decoupling group. This is the reason why we choose the Hamiltonian in Eq. (1).

3 The scheme

We first realize one-qubit gates and then realize a nontrivial two-qubit gate. By combining them, universal quantum computation can be realized.

To start with, we realize dynamical-decoupling-protected nonadiabatic geometric one-qubit gates. For this, we encode the logical qubit as $\{|0\rangle_L = |010\rangle, |1\rangle_L = |100\rangle\}$, where $|abc\rangle \equiv |a\rangle \otimes |b\rangle \otimes |c\rangle$ $(a, b, c \in \{0, 1\})$. Here, the third qubit is used as an auxiliary qubit, which plays an important role in performing operations on the logical qubit. The one-qubit gate we aim to realize is

$$U = \mathrm{e}^{-\mathrm{i}\phi(\cos\varphi X_L + \sin\varphi Y_L)/2}, \tag{6}$$

where ϕ and φ are time-independent parameters, and $X_L(Y_L, Z_L)$ is the Pauli $x(y, z)$ operator acting on $|0\rangle_L$ and $|1\rangle_L$. This is a quantum gate about a rotation axis in the x–y plane. By combining two such quantum gates, an arbitrary one-qubit gate can be realized.

To complete our realization, we divide the whole evolution into three intervals. The nonzero parameters in the intervals $t \in [0, \tau_1] \cup (\tau_2, \tau]$ are set to be $J^z_{13} = J(t)$ and in the interval $t \in (\tau_1, \tau_2]$ are set to be $J^{xy}_{12} = J(t)\sin(\phi/2)$ and $J^z_{13} = -J(t)\cos(\phi/2)$, where $J(t)$ is time dependent. In this case, the Hamiltonian in Eq. (1) reads

$$\begin{aligned} H_1(t) =& J(t)R^z_{13}, \quad t \in [0, \tau_1] \cup (\tau_2, \tau], \\ H_2(t) =& J(t)\left(\sin\frac{\phi}{2}R^{xy}_{12} - \cos\frac{\phi}{2}R^z_{13}\right), \quad t \in (\tau_1, \tau_2]. \end{aligned} \tag{7}$$

If the parameter $J(t)$ is required to satisfy

$$\begin{aligned} &\int_0^{\tau_1} J(t)\mathrm{d}t = \frac{\pi}{4} - \frac{\varphi}{2}, \quad \int_{\tau_1}^{\tau_2} J(t)\mathrm{d}t = \frac{\pi}{2}, \\ &\int_{\tau_2}^{\tau} J(t)\mathrm{d}t = \frac{\pi}{4} + \frac{\varphi}{2}, \end{aligned} \tag{8}$$

the evolution operator after the whole evolution, in the basis $\{|0\rangle_L, |1\rangle_L\}$, reads

$$U(\tau) = \begin{pmatrix} \cos\frac{\phi}{2} & -\mathrm{i}\sin\frac{\phi}{2}\mathrm{e}^{-\mathrm{i}\varphi} \\ -\mathrm{i}\sin\frac{\phi}{2}\mathrm{e}^{\mathrm{i}\varphi} & \cos\frac{\phi}{2} \end{pmatrix}. \tag{9}$$

It is just the matrix representation of Eq. (6). In the following, we show that the above quantum gate is a nonadiabatic geometric gate.

For this purpose, we examine the evolution of a quantum state starting from one of the orthonormal vectors

$$\begin{aligned} |\psi_+\rangle =& \frac{1}{\sqrt{2}}(|0\rangle_L + \mathrm{e}^{\mathrm{i}\varphi}|1\rangle_L), \\ |\psi_-\rangle =& \frac{1}{\sqrt{2}}(\mathrm{e}^{-\mathrm{i}\varphi}|0\rangle_L - |1\rangle_L). \end{aligned} \tag{10}$$

We can find that the quantum state satisfies the cyclic evolution condition, $|\psi_+(\tau)\rangle = U(\tau)|\psi_+\rangle = \exp(-\mathrm{i}\phi/2)|\psi_+\rangle$ or $|\psi_-(\tau)\rangle = U(\tau)|\psi_-\rangle = \exp(\mathrm{i}\phi/2)|\psi_-\rangle$. Furthermore, we can verify that the quantum system satisfies the parallel transport condition, $\langle\psi_\pm(t)|H_1(t)|\psi_\pm(t)\rangle = 0$ $(t \in [0, \tau_1] \cup (\tau_2, \tau])$ and $\langle\psi_\pm(t)|H_2(t)|\psi_\pm(t)\rangle = 0$ $(t \in (\tau_1, \tau_2])$, too. Therefore, $\phi/2$ and $-\phi/2$ are purely geometric phases and the quantum gate in Eq. (9) is a nonadiabatic geometric gate. Here, we would like to point out that our scheme is based on Abelian geometric phases and thus one only needs to make the diagonal elements vanish for satisfying the parallel transport condition. This is different from the scheme based on non-Abelian geometric phases [69, 70], in which one needs to make both diagonal and off-diagonal elements vanish for satisfying the parallel transport condition.

We have realized one-qubit nonadiabatic geometric gates. To realize universal quantum computation, we also need a nontrivial two-qubit gate. Next, we demonstrate how to realize a nontrivial two-qubit nonadiabatic geometric gate protected by dynamical decoupling.

To be compatible with the one-logical-qubit encode, we encode the two logical qubits as $\{|00\rangle_L = |010010\rangle, |01\rangle_L = |010100\rangle, |10\rangle_L = |100010\rangle, |11\rangle_L = |100100\rangle\}$. Similarly to the one-qubit gates, we realize the two-qubit gate by dividing the whole evolution into three intervals. In the intervals $t \in [0,\tau_1]\cup(\tau_2,\tau]$, the nonzero parameter is set to be $J^z_{25}=\lambda(t)$, and in the interval $t\in(\tau_1,\tau_2]$, the nonzero parameters are set to be $J^{xy}_{45}=\lambda(t)\sin(\kappa/2)$ and $J^z_{25}=-\lambda(t)\cos(\kappa/2)$. Here, $\lambda(t)$ is time dependent and κ is time independent. As a result, the Hamiltonian in Eq. (1) reads

$$\begin{aligned} H_1(t) =&\lambda(t)R^z_{25}, \quad t\in[0,\tau_1]\cup(\tau_2,\tau],\\ H_2(t) =&\lambda(t)\left(\sin\frac{\kappa}{2}R^{xy}_{45}-\cos\frac{\kappa}{2}R^z_{25}\right), \quad t\in(\tau_1,\tau_2]. \end{aligned} \tag{11}$$

If the parameter $\lambda(t)$ is set to satisfy

$$\begin{aligned} &\int_0^{\tau_1}\lambda(t)\mathrm{d}t=\frac{\pi}{4}-\frac{\epsilon}{2}, \quad \int_{\tau_1}^{\tau_2}\lambda(t)\mathrm{d}t=\frac{\pi}{2},\\ &\int_{\tau_2}^{\tau}\lambda(t)\mathrm{d}t=\frac{\pi}{4}+\frac{\epsilon}{2} \end{aligned} \tag{12}$$

with ϵ being a time-independent parameter, the evolution operator at the final time, in the basis $\{|00\rangle_L, |01\rangle_L, |10\rangle_L, |11\rangle_L\}$, reads

$$U(\tau)=\begin{pmatrix} \cos\frac{\kappa}{2} & -\mathrm{i}\sin\frac{\kappa}{2}\mathrm{e}^{-\mathrm{i}\epsilon} & 0 & 0\\ -\mathrm{i}\sin\frac{\kappa}{2}\mathrm{e}^{\mathrm{i}\epsilon} & \cos\frac{\kappa}{2} & 0 & 0\\ 0 & 0 & \cos\frac{\kappa}{2} & -\mathrm{i}\sin\frac{\kappa}{2}\mathrm{e}^{\mathrm{i}\epsilon}\\ 0 & 0 & -\mathrm{i}\sin\frac{\kappa}{2}\mathrm{e}^{-\mathrm{i}\epsilon} & \cos\frac{\kappa}{2} \end{pmatrix}. \tag{13}$$

This is a nontrivial two-qubit gate. In the following, we show that this quantum gate is a nonadiabatic geometric gate.

First, we can verify that a quantum state starting from one of the orthonormal vectors

$$\begin{aligned} |\Psi_+\rangle =&\frac{1}{\sqrt{2}}(|00\rangle_L+\mathrm{e}^{\mathrm{i}\epsilon}|01\rangle_L),\\ |\Psi_-\rangle =&\frac{1}{\sqrt{2}}(|00\rangle_L-\mathrm{e}^{\mathrm{i}\epsilon}|01\rangle_L),\\ |\Phi_+\rangle =&\frac{1}{\sqrt{2}}(|10\rangle_L+\mathrm{e}^{-\mathrm{i}\epsilon}|11\rangle_L),\\ |\Phi_-\rangle =&\frac{1}{\sqrt{2}}(|10\rangle_L-\mathrm{e}^{-\mathrm{i}\epsilon}|11\rangle_L) \end{aligned} \tag{14}$$

undergoes cyclic evolution, $|\Psi_+(\tau)\rangle = U(\tau)|\Psi_+\rangle = \exp(-\mathrm{i}\kappa/2)|\Psi_+\rangle$, $|\Psi_-(\tau)\rangle = U(\tau)|\Psi_-\rangle = \exp(\mathrm{i}\kappa/2)|\Psi_-\rangle$, $|\Phi_+(\tau)\rangle = U(\tau)|\Phi_+\rangle = \exp(-\mathrm{i}\kappa/2)|\Phi_+\rangle$, and $|\Phi_-(\tau)\rangle = U(\tau)|\Phi_-\rangle = \exp(\mathrm{i}\kappa/2)|\Phi_-\rangle$, i.e., the cyclic evolution condition is satisfied. Second, we can verify that $\langle\Psi_\pm(t)|H_1(t)|\Psi_\pm(t)\rangle = 0$ $(t\in[0,\tau_1]\cup(\tau_2,\tau])$, $\langle\Psi_\pm(t)|H_2(t)|\Psi_\pm(t)\rangle = 0$ $(t\in(\tau_1,\tau_2])$, $\langle\Phi_\pm(t)|H_1(t)|\Phi_\pm(t)\rangle = 0$ $(t\in[0,\tau_1]\cup(\tau_2,\tau])$, and $\langle\Phi_\pm(t)|H_2(t)|\Phi_\pm(t)\rangle = 0$ $(t\in(\tau_1,\tau_2])$, i.e., the parallel transport condition is satisfied. Therefore, the acquired phases are purely geometric phases and the quantum gate in Eq. (13) is a nonadiabatic geometric gate.

4 The flexibility of our physical model

We have realized a universal set of dynamical-decoupling-protected nonadiabatic geometric gates, where one-qubit gates are those about a rotation axis in the x–y plane. It is interesting to note that our physical model also allows one to realize the one-qubit gates about a rotation axis in the y–z plane or x–z plane, which can also perform universal quantum computation by combining with the realized two-qubit gate. This increases the flexibility for the realization of universal nonadiabatic geometric gates protected by dynamical decoupling. We below demonstrate how to realize the one-qubit gates about rotation axes in the y–z plane and x–z plane.

First, we realize the one-qubit gate about a rotation axis in the y–z plane,

$$U=\mathrm{e}^{-\mathrm{i}\phi(\sin\theta Y_L+\cos\theta Z_L)/2} \tag{15}$$

with θ and ϕ being time-independent parameters. To complete the realization, we divide the whole evolution into three intervals. In the intervals $t\in[0,\tau_1]\cup(\tau_2,\tau]$, the nonzero parameter is set to be $J^{xy}_{12}=-J(t)$, and in the interval $t\in(\tau_1,\tau_2]$, the nonzero parameters are set to be $J^{xy}_{12}=J(t)\cos(\phi/2)$ and $J^z_{13}=J(t)\sin(\phi/2)$. Consequently, the Hamiltonian in Eq. (1) reads

$$\begin{aligned} H_1(t) =&-J(t)R^{xy}_{12}, \quad t\in[0,\tau_1]\cup(\tau_2,\tau],\\ H_2(t) =&J(t)\left(\cos\frac{\phi}{2}R^{xy}_{12}+\sin\frac{\phi}{2}R^z_{13}\right), \quad t\in(\tau_1,\tau_2]. \end{aligned} \tag{16}$$

If we require $J(t)$ to satisfy

$$\begin{aligned} &\int_0^{\tau_1}J(t)\mathrm{d}t=\frac{\pi}{4}-\frac{\theta}{2}, \quad \int_{\tau_1}^{\tau_2}J(t)\mathrm{d}t=\frac{\pi}{2},\\ &\int_{\tau_2}^{\tau}J(t)\mathrm{d}t=\frac{\pi}{4}+\frac{\theta}{2}, \end{aligned} \tag{17}$$

the evolution operator, in the basis $\{|0\rangle_L, |1\rangle_L\}$, reads

$$U(\tau)=\begin{pmatrix} \cos\frac{\phi}{2}-\mathrm{i}\sin\frac{\phi}{2}\cos\theta & -\sin\frac{\phi}{2}\sin\theta\\ \sin\frac{\phi}{2}\sin\theta & \cos\frac{\phi}{2}+\mathrm{i}\sin\frac{\phi}{2}\cos\theta \end{pmatrix}. \tag{18}$$

This is just the quantum gate in Eq. (15). To show the above quantum gate is a nonadiabatic geometric gate, we examine the evolution of a quantum state starting from one of the orthonormal vectors

$$|\psi_+\rangle = \cos\frac{\theta}{2}|0\rangle_L + \mathrm{i}\sin\frac{\theta}{2}|1\rangle_L,$$
$$|\psi_-\rangle = -\mathrm{i}\sin\frac{\theta}{2}|0\rangle_L - \cos\frac{\theta}{2}|1\rangle_L. \quad (19)$$

We can verify that the quantum state satisfies the cyclic evolution condition, $|\psi_+(\tau)\rangle = U(\tau)|\psi_+\rangle = \exp(-\mathrm{i}\phi/2)|\psi_+\rangle$ or $|\psi_-(\tau)\rangle = U(\tau)|\psi_-\rangle = \exp(\mathrm{i}\phi/2)|\psi_-\rangle$. Furthermore, we can verify that the quantum system satisfies the parallel transport condition, $\langle\psi_\pm(t)|H_1(t)|\psi_\pm(t)\rangle = 0$ $(t\in[0,\tau_1]\cup(\tau_2,\tau])$ and $\langle\psi_\pm(t)|H_2(t)|\psi_\pm(t)\rangle = 0$ $(t\in(\tau_1,\tau_2])$, too. Therefore, $\phi/2$ and $-\phi/2$ are purely geometric phases and the quantum gate in Eq. (18) is a nonadiabatic geometric gate.

Second, we realize the one-qubit gate about a rotation axis in the x–z plane,

$$U = \mathrm{e}^{-\mathrm{i}\phi(\sin\theta X_L+\cos\theta Z_L)/2}. \quad (20)$$

To complete the realization, we also divide the whole evolution into three intervals. In the intervals $t\in[0,\tau_1]\cup(\tau_2,\tau]$, we set the nonzero parameters as $J_{12}^{xy} = -J(t)\cos\theta$ and $J_{13}^{z} = J(t)\sin\theta$, and in the interval $t\in(\tau_1,\tau_2]$, we set the nonzero parameters as $J_{12}^{xy} = J(t)\cos(\theta-\phi/2)$ and $J_{13}^{z} = -J(t)\sin(\theta-\phi/2)$. As a result, the Hamiltonians in Eq. (1) reads

$$H_1(t) = J(t)(\sin\theta R_{13}^z - \cos\theta R_{12}^{xy}), \quad t\in[0,\tau_1]\cup(\tau_2,\tau],$$
$$H_2(t) = J(t)\left[\cos\left(\theta-\frac{\phi}{2}\right)R_{12}^{xy} - \sin\left(\theta-\frac{\phi}{2}\right)R_{13}^{z}\right] \quad t\in(\tau_1,\tau_2]. \quad (21)$$

If we require $J(t)$ to satisfy

$$\int_0^{\tau_1} J(t)\mathrm{d}t = \int_{\tau_2}^{\tau} J(t)\mathrm{d}t = \frac{\pi}{4}, \quad \int_{\tau_1}^{\tau_2} J(t)\mathrm{d}t = \frac{\pi}{2}, \quad (22)$$

the evolution operator, in the basis $\{|0\rangle_L, |1\rangle_L\}$, reads

$$U(\tau) = \begin{pmatrix} \cos\frac{\phi}{2} - \mathrm{i}\sin\frac{\phi}{2}\cos\theta & -\mathrm{i}\sin\frac{\phi}{2}\sin\theta \\ -\mathrm{i}\sin\frac{\phi}{2}\sin\theta & \cos\frac{\phi}{2} + \mathrm{i}\sin\frac{\phi}{2}\cos\theta \end{pmatrix}. \quad (23)$$

This is just the quantum gate in Eq. (20). Similarly to the demonstration of the gate in Eq. (9) or Eq. (18) being a nonadiabatic geometric gate, we can show that the quantum gate in Eq. (23) is a nonadiabatic geometric gate, too.

5 Numerical simulations

In this section, we specifically demonstrate the performance of nonadiabatic geometric gates being protected by dynamical decoupling with the aid of numerical simulations. For this purpose, we use the fidelity

$$F = \langle\psi(\tau)|\rho(\tau)|\psi(\tau)\rangle \quad (24)$$

to characterize the performance of quantum gates. Here, $|\psi(\tau)\rangle$ is the ideal final state obtained by applying the quantum gate $U(\tau)$ to the initial state $|\psi(0)\rangle$, and $\rho(\tau)$ is the density operator describing a real final state. To calculate $\rho(\tau)$, we first solve the Liouville equation

$$\dot{\rho}_{\mathrm{SE}}(t) = -\mathrm{i}[H_{\mathrm{tot}}(t), \rho_{\mathrm{SE}}(t)], \quad (25)$$

and then perform a partial trace over the environment, where $\rho_{\mathrm{SE}}(t)$ is the density operator of the joint system and $H_{\mathrm{tot}}(t) = H(t) + H_I + H_E$ is the total Hamiltonian. In this way, the reduced state $\rho(t)$ can be obtained as

$$\rho(t) = \mathrm{tr}_{\mathrm{E}}\rho_{\mathrm{SE}}(t). \quad (26)$$

In our numerical simulations, we take one-qubit gate $U(\tau) = \exp(-\mathrm{i}\pi X_L/2)$ and two-qubit gate $U(\tau) = |0\rangle_{LL}\langle 0|\otimes\exp(-\mathrm{i}\pi Y_L/4) + |1\rangle_{LL}\langle 1|\otimes\exp(\mathrm{i}\pi Y_L/4)$ as examples to illustrate the performance, where the quantum gates are obtained by using the method in Section 3 .

For the one-qubit gate, we choose the initial states as $|\psi(0)\rangle = (|0\rangle_L + |1\rangle_L)/\sqrt{2}$ and $|\psi(0)\rangle = (|0\rangle_L - |1\rangle_L)/\sqrt{2}$, and the environment Hamiltonian and interaction Hamiltonian as $H_E = J'(\sum_{k=1}^{3} I_k)\otimes\sigma_x$ and $H_I = J'[\sum_{k=1}^{3}(\sigma_k^x + \sigma_k^y + \sigma_k^z)]\otimes\sigma_x$ with $J = 25J' = 2\pi\times 5\mathrm{MHz}$. In Figs. 2(a), (b), (c), and (d), we plot the populations $P(t) = \langle\psi(\tau)|\rho(t)|\psi(\tau)\rangle$ as a function of time t with initial state $|\psi(0)\rangle = (|0\rangle_L + |1\rangle_L)/\sqrt{2}$. In Figs. 3(a), (b), (c), and (d), we plot the populations $P(t) = \langle\psi(\tau)|\rho(t)|\psi(\tau)\rangle$ as a function of time t with initial state $|\psi(0)\rangle = (|0\rangle_L - |1\rangle_L)/\sqrt{2}$. Here, the fidelities of the final states can be obtained as $F = P(\tau)$. In Figs. 2(a) and 3(a), we do not use the dynamical decoupling to protect the quantum gate. In Figs. 2(b) and 3(b), we apply three sequences with decoupling operations $\{\otimes_{k=1}^{3} I_k, \otimes_{k=1}^{3}\sigma_k^x, \otimes_{k=1}^{3}\sigma_k^y, \otimes_{k=1}^{3}\sigma_k^z\}$ to the quantum system, each of which operates in a different interval $t\in[0,\tau_1]$, $t\in(\tau_1,\tau_2]$, or $t\in(\tau_2,\tau]$. In Figs. 2(c) and 3(c), we apply six sequences to the quantum system, and in each interval we apply two sequences to the quantum system. In Figs. 2(d) and 3(d), we apply twelve sequences to the quantum system, and in each interval we apply four sequences to the quantum system. The simulations show that the fidelities of the final states in Figs. 2(a), (b), (c), and (d) are respectively 93.10%, 99.83%, 99.96%, and 99.99%, and the fidelities of the final states in Figs. 3(a), (b), (c), and (d) are respectively 95.19%, 99.97%, 99.99%, and 100%.

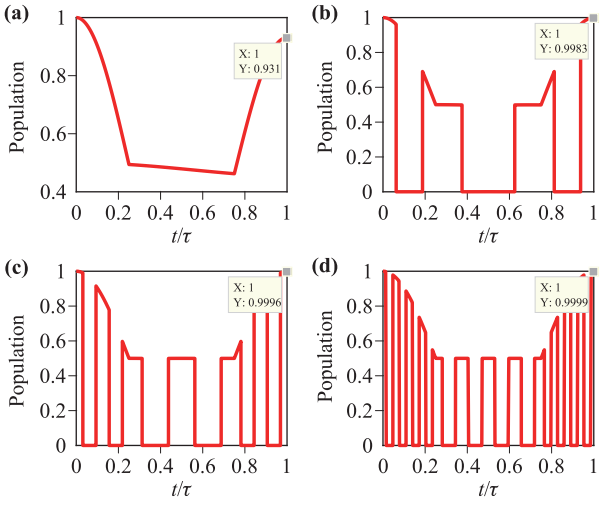

Fig. 2 The populations $P(t) = \langle\psi(\tau)|\,\rho(t)\,|\psi(\tau)\rangle$ as a function of time t (units of τ). Here, $|\psi(\tau)\rangle = U(\tau)\,|\psi(0)\rangle$ is an ideal final state, $\rho(t)$ is a real evolution state, $U(\tau) = \exp(-\mathrm{i}\pi X_L/2)$ is the chosen quantum gate, and $|\psi(0)\rangle = (|0\rangle_L + |1\rangle_L)/\sqrt{2}$ is the chosen initial state. **(a)** The population without being protected by dynamical decoupling. **(b)** The population with applying three sequences to the quantum system. **(c)** The population with applying six sequences to the quantum system. **(d)** The population with applying twelve sequences to the quantum system.

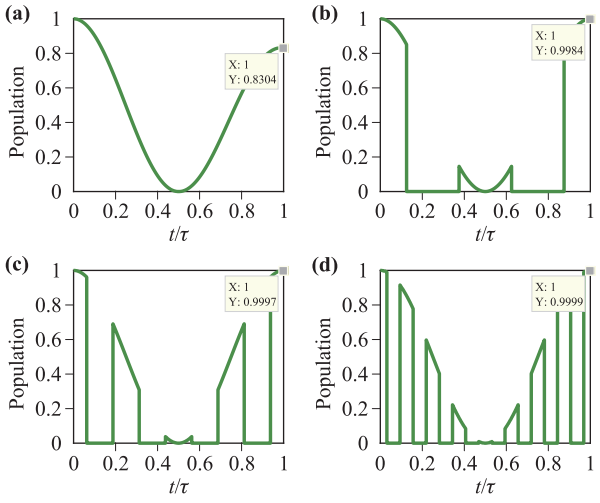

Fig. 4 The populations $P(t) = \langle\psi(\tau)|\,\rho(t)\,|\psi(\tau)\rangle$ as a function of time t (units of τ). Here, $|\psi(\tau)\rangle = U(\tau)\,|\psi(0)\rangle$ is an ideal final state with $U(\tau) = |0\rangle_{LL}\langle 0| \otimes \exp(-\mathrm{i}\pi Y_L/4) + |1\rangle_{LL}\langle 1| \otimes \exp(\mathrm{i}\pi Y_L/4)$ and $|\psi(0)\rangle = (|00\rangle_L + \mathrm{i}\,|01\rangle_L)/\sqrt{2}$, and $\rho(t)$ is a real evolution state.**(a)** The population without being protected by dynamical decoupling. **(b)** The population with applying two sequences to the quantum system. **(c)** The population with applying four sequences to the quantum system. **(d)** The population with applying eight sequences to the quantum system.

For the two-qubit gates, we choose the initial state as $|\psi(0)\rangle = (|00\rangle_L + \mathrm{i}\,|01\rangle_L)/\sqrt{2}$, and the environment Hamiltonian and interaction Hamiltonian as $H_E = \lambda'(\sum_{k=1}^{6} I_k) \otimes \sigma_x$ and $H_I = \lambda'[\sum_{k=1}^{6}(\sigma_k^x + \sigma_k^y + \sigma_k^z)] \otimes \sigma_x$ with $\lambda = 25\lambda' = 2\pi \times 5\mathrm{MHz}$. We plot the populations $P(t) = \langle\psi(\tau)|\,\rho(t)\,|\psi(\tau)\rangle$ as a function of time t in Figs. 4(a), (b), (c), and (d). In Fig. 4(a), we do not use the dynamical decoupling to protect the quantum gate. In Fig. 4(b), we apply two sequences with decoupling operations $\{\otimes_{k=1}^{6} I_k, \otimes_{k=1}^{6}\sigma_k^x, \otimes_{k=1}^{6}\sigma_k^y, \otimes_{k=1}^{6}\sigma_k^z\}$ to the quantum system, each of which operates in a different interval $t \in [0, \tau_2]$ or $t \in (\tau_2, \tau]$ ($\tau_1 = 0$). In Fig. 4(c), we apply four sequences to the quantum system, and in each interval we apply two sequences to the quantum system. In Fig. 4(d), we apply eight sequences to the quantum system, and in each interval we apply four sequences to the quantum system. The simulations show that the fidelities of the final states in Figs. 4(a), (b), (c), and (d) are 83.04%, 99.84%, 99.97%, and 99.99%, respectively.

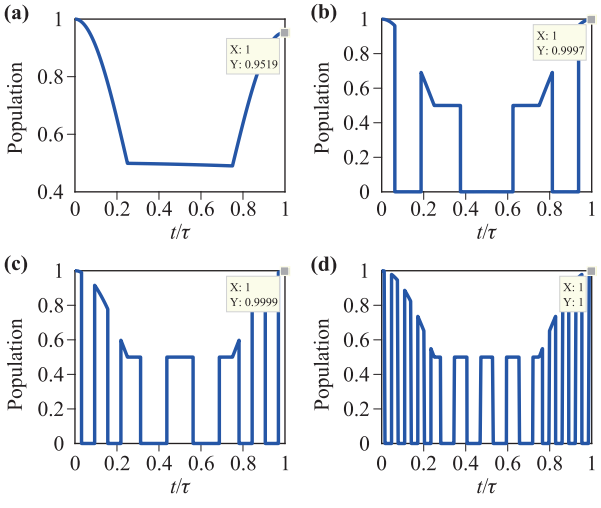

Fig. 3 The populations $P(t) = \langle\psi(\tau)|\,\rho(t)\,|\psi(\tau)\rangle$ as a function of time t (units of τ). Here, $|\psi(\tau)\rangle = U(\tau)\,|\psi(0)\rangle$ is an ideal final state with $U(\tau) = \exp(-\mathrm{i}\pi X_L/2)$ and $|\psi(0)\rangle = (|0\rangle_L - |1\rangle_L)/\sqrt{2}$, and $\rho(t)$ is a real evolution state. **(a)** The population without being protected by dynamical decoupling. **(b)** The population with applying three sequences to the quantum system. **(c)** The population with applying six sequences to the quantum system. **(d)** The population with applying twelve sequences to the quantum system.

6 Conclusion

In conclusion, we have proposed a scheme of nonadiabatic geometric quantum computation protected by dynamical decoupling, which is based on the XXZ Hamiltonian. Since the XXZ Hamiltonian can be realized in a number of

solid-state systems, such as superconducting circuits and quantum dots, our scheme provides an effective method for the implementation of dynamical-decoupling-protected nonadiabatic geometric gates with solid-state systems. In addition, we have demonstrated that our scheme allows one to realize not only the one-qubit gates about a rotation axis in the x–y plane but also the one-qubit gates about a rotation axis in the y–z plane or x–z plane, indicating the flexibility of our scheme for the realization of universal gates. With the aid of numerical simulations, we have demonstrated the performance of our scheme. The result shows that dynamical decoupling indeed protects nonadiabatic geometric gate against the environment-induced decoherence.

Acknowledgements We acknowledge support from the National Natural Science Foundation of China under Grant No. 11947221 and the China Postdoctoral Science Foundation under Grant No. 2019M662318.

References

1. P. W. Shor, Polynomial-time algorithms for prime factorization and discrete logarithms on a quantum computer, *SIAM J. Comput.* 26(5), 1484 (1997)
2. L. K. Grover, Quantum mechanics helps in searching for a needle in a haystack, *Phys. Rev. Lett.* 79(2), 325 (1997)
3. M. J. Bremner, C. M. Dawson, J. L. Dodd, A. Gilchrist, A. W. Harrow, D. Mortimer, M. A. Nielsen, and T. J. Osborne, Practical scheme for quantum computation with any two-qubit entangling gate, *Phys. Rev. Lett.* 89(24), 247902 (2002)
4. M. V. Berry, Quantal phase factors accompanying adiabatic changes, *Proc. R. Soc. Lond. A* 392(1802), 45 (1984)
5. F. Wilczek and A. Zee, Appearance of gauge structure in simple dynamical systems, *Phys. Rev. Lett.* 52(24), 2111 (1984)
6. J. A. Jones, V. Vedral, A. Ekert, and G. Castagnoli, Geometric quantum computation using nuclear magnetic resonance, *Nature* 403(6772), 869 (2000)
7. P. Zanardi and M. Rasetti, Holonomic quantum computation, *Phys. Lett. A* 264(2–3), 94 (1999)
8. L. M. Duan, J. I. Cirac, and P. Zoller, Geometric manipulation of trapped ions for quantum computation, *Science* 292(5522), 1695 (2001)
9. M. Born and V. Fock, Beweis des adiabatensatzes, *Z. Phys.* 51(3–4), 165 (1928)
10. A. Messiah, Quantum Mechanics, North-Holland, Amsterdam, Vol. 2, 1962
11. D. M. Tong, Quantitative condition is necessary in guaranteeing the validity of the adiabatic approximation, *Phys. Rev. Lett.* 104(12), 120401 (2010)
12. X. B. Wang and M. Keiji, Nonadiabatic conditional geometric phase shift with NMR, *Phys. Rev. Lett.* 87(9), 097901 (2001)
13. S. L. Zhu and Z. D. Wang, Implementation of universal quantum gates based on nonadiabatic geometric phases, *Phys. Rev. Lett.* 89(9), 097902 (2002)
14. Y. Aharonov and J. Anandan, Phase change during a cyclic quantum evolution, *Phys. Rev. Lett.* 58(16), 1593 (1987)
15. E. Sjöqvist, D. M. Tong, L. Mauritz Andersson, B. Hessmo, M. Johansson, and K. Singh, Non-adiabatic holonomic quantum computation, *New J. Phys.* 14(10), 103035 (2012)
16. G. F. Xu, J. Zhang, D. M. Tong, E. Sjöqvist, and L. C. Kwek, Nonadiabatic holonomic quantum computation in decoherence-free subspaces, *Phys. Rev. Lett.* 109(17), 170501 (2012)
17. J. Anandan, Non-adiabatic non-abelian geometric phase, *Phys. Lett. A* 133(4–5), 171 (1988)
18. S. L. Zhu and Z. D. Wang, Unconventional geometric quantum computation, *Phys. Rev. Lett.* 91(18), 187902 (2003)
19. A. Friedenauer and E. Sjöqvist, Noncyclic geometric quantum computation, *Phys. Rev. A* 67(2), 024303 (2003)
20. P. Solinas, P. Zanardi, N. Zanghì, and F. Rossi, Nonadiabatic geometrical quantum gates in semiconductor quantum dots, *Phys. Rev. A* 67(5), 052309 (2003)
21. S. B. Zheng, Unconventional geometric quantum phase gates with a cavity QED system, *Phys. Rev. A* 70(5), 052320 (2004)
22. X. D. Zhang, S. L. Zhu, L. Hu, and Z. D. Wang, Nonadiabatic geometric quantum computation using a single-loop scenario, *Phys. Rev. A* 71(1), 014302 (2005)
23. C. Y. Chen, M. Feng, X. L. Zhang, and K. L. Gao, Strong-driving-assisted unconventional geometric logic gate in cavity QED, *Phys. Rev. A* 73(3), 032344 (2006)
24. L. X. Cen, Z. D. Wang, and S. J. Wang, Scalable quantum computation in decoherence-free subspaces with trapped ions, *Phys. Rev. A* 74(3), 032321 (2006)
25. X. L. Feng, Z. S. Wang, C. F. Wu, L. C. Kwek, C. H. Lai, and C. H. Oh, Scheme for unconventional geometric quantum computation in cavity QED, *Phys. Rev. A* 75(5), 052312 (2007)
26. C. F. Wu, Z. S. Wang, X. L. Feng, H. S. Goan, L. C. Kwek, C. H. Lai, and C. H. Oh, Unconventional geometric quantum computation in a two-mode cavity, *Phys. Rev. A* 76(2), 024302 (2007)
27. K. Kim, C. F. Roos, L. Aolita, H. Häffner, V. Nebendahl, and R. Blatt, Geometric phase gate on an optical transition for ion trap quantum computation, *Phys. Rev. A* 77, 050303(R) (2008)
28. X. L. Feng, C. F. Wu, H. Sun, and C. H. Oh, Geometric entangling gates in decoherence-free subspaces with minimal requirements, *Phys. Rev. Lett.* 103(20), 200501 (2009)
29. Y. Ota and Y. Kondo, Composite pulses in NMR as nonadiabatic geometric quantum gates, *Phys. Rev. A* 80(2), 024302 (2009)
30. J. T. Thomas, M. Lababidi, and M. Z. Tian, Robustness of single-qubit geometric gate against systematic error, *Phys. Rev. A* 84(4), 042335 (2011)

31. G. F. Xu and G. L. Long, Protecting geometric gates by dynamical decoupling, *Phys. Rev. A* 90(2), 022323 (2014)
32. X. Wu and P. Z. Zhao, Universal nonadiabatic geometric gates protected by dynamical decoupling, *Phys. Rev. A* 102(3), 032627 (2020)
33. C. F. Sun, G. C. Wang, C. F. Wu, H. D. Liu, X. L. Feng, J. L. Chen, and K. Xue, Non-adiabatic holonomic quantum computation in linear system-bath coupling, *Sci. Rep.* 6(1), 20292 (2016)
34. G. F. Xu and G. L. Long, Universal nonadiabatic geometric gates in two-qubit decoherence-free subspaces, *Sci. Rep.* 4(1), 6814 (2015)
35. P. Z. Zhao, G. F. Xu, and D. M. Tong, Nonadiabatic geometric quantum computation in decoherence-free subspaces based on unconventional geometric phases, *Phys. Rev. A* 94(6), 062327 (2016)
36. P. Z. Zhao, X. D. Cui, G. F. Xu, E. Sjöqvist, and D. M. Tong, Rydberg-atom-based scheme of nonadiabatic geometric quantum computation, *Phys. Rev. A* 96(5), 052316 (2017)
37. T. Chen and Z. Y. Xue, Nonadiabatic geometric quantum computation with parametrically tunable coupling, *Phys. Rev. Appl.* 10(5), 054051 (2018)
38. B. J. Liu, X. K. Song, Z. Y. Xue, X. Wang, and M. H. Yung, Plug-and-play approach to nonadiabatic geometric quantum gates, *Phys. Rev. Lett.* 123(10), 100501 (2019)
39. Y. H. Kang, Z. C. Shi, B. H. Huang, J. Song, and Y. Xia, Flexible scheme for the implementation of nonadiabatic geometric quantum computation, *Phys. Rev. A* 101(3), 032322 (2020)
40. Y. H. Kang and Y. Xia, Unconventional geometric phase gate of transmon qubits with inverse Hamiltonian engineering, *IEEE J. Sel. Top. Quantum Electron.* 26(3), 6700107 (2020)
41. K. Z. Li, P. Z. Zhao, and D. M. Tong, Approach to realizing nonadiabatic geometric gates with prescribed evolution paths, *Phys. Rev. Res.* 2(2), 023295 (2020)
42. J. Xu, S. Li, T. Chen, and Z. Y. Xue, Nonadiabatic geometric quantum computation with optimal control on superconducting circuits, *Front. Phys.* 15(4), 41503 (2020)
43. F. Q. Guo, J. L. Wu, X. Y. Zhu, Z. Jin, Y. Zeng, S. Zhang, L. L. Yan, M. Feng, and S. L. Su, Complete and nondestructive distinguishment of many-body Rydberg entanglement via robust geometric quantum operations, *Phys. Rev. A* 102(6), 062410 (2020)
44. M. R. Yun, F. Q. Guo, M. Li, L. L. Yan, M. Feng, Y. X. Li, and S. L. Su, Distributed geometric quantum computation based on the optimized-control-technique in a cavity-atom system via exchanging virtual photons, *Opt. Express* 29(6), 8737 (2021)
45. D. Leibfried, B. DeMarco, V. Meyer, D. Lucas, M. Barrett, J. Britton, W. M. Itano, B. Jelenković, C. Langer, T. Rosenband, and D. J. Wineland, Experimental demonstration of a robust, high-fidelity geometric two ion-qubit phase gate, *Nature* 422(6930), 412 (2003)
46. J. F. Du, P. Zou, and Z. D. Wang, Experimental implementation of high-fidelity unconventional geometric quantum gates using an NMR interferometer, *Phys. Rev. A* 74, 020302(R) (2006)
47. P. Z. Zhao, Z. J. Z. Dong, Z. X. Zhang, G. P. Guo, D. M. Tong, and Y. Yin, Experimental realization of nonadiabatic geometric gates with a superconducting Xmon qubit, *Sci. China Phys. Mech. Astron.* 64(5), 250362 (2021)
48. Y. Xu, Z. Hua, T. Chen, X. Pan, X. Li, J. Han, W. Cai, Y. Ma, H. Wang, Y. P. Song, Z. Y. Xue, and L. Sun, Experimental implementation of universal nonadiabatic geometric quantum gates in a superconducting circuit, *Phys. Rev. Lett.* 124(23), 230503 (2020)
49. L. Viola, E. Knill, and S. Lloyd, Dynamical decoupling of open quantum systems, *Phys. Rev. Lett.* 82(12), 2417 (1999)
50. C. N. Yang and C. P. Yang, One-dimensional chain of anisotropic spin-spin interactions (I): Proof of Bethe's hypothesis for ground state in a finite system, *Phys. Rev.* 150(1), 321 (1966)
51. J. D. Johnson and M. McCoy, Low-temperature thermodynamics of the $|\Delta| \geq 1$ Heisenberg-Ising ring, *Phys. Rev. A* 6(4), 1613 (1972)
52. F. C. Alcaraz and A. L. Malvezzi, Critical and off-critical properties of the *XXZ* chain in external homogeneous and staggered magnetic fields, *J. Phys. A* 28(6), 1521 (1995)
53. N. Canosa and R. Rossignoli, Global entanglement in *XXZ* chains, *Phys. Rev. A* 73(2), 022347 (2006)
54. O. Breunig, M. Garst, E. Sela, B. Buldmann, P. Becker, L. Bohaty, R. Müller, and T. Lorenz, Spin-1/2 *XXZ* chain system Cs_2CoCl_4 in a transverse magnetic field, *Phys. Rev. Lett.* 111(18), 187202 (2013)
55. U. Glaser, H. Büttner, and H. Fehske, Entanglement and correlation in anisotropic quantum spin systems, *Phys. Rev. A* 68(3), 032318 (2003)
56. E. Altman, W. Hofstetter, E. Demler, and M. D. Lukin, Phase diagram of two-component bosons on an optical lattice, *New J. Phys.* 5, 113 (2003)
57. J. Zhou, Y. Hu, X. B. Zou, and G. C. Guo, Ground-state preparation of arbitrarily multipartite Dicke states in the one-dimensional ferromagnetic spin-1/2 chain, *Phys. Rev. A* 84(4), 042324 (2011)
58. A. V. Gorshkov, S. R. Manmana, G. Chen, J. Ye, E. Demler, M. D. Lukin, and A. M. Rey, Tunable superfluidity and quantum magnetism with ultracold polar molecules, *Phys. Rev. Lett.* 107(11), 115301 (2011)
59. A. V. Gorshkov, S. R. Manmana, G. Chen, E. Demler, M. D. Lukin, and A. M. Rey, Quantum magnetism with polar alkali-metal dimers, *Phys. Rev. A* 84(3), 033619 (2011)
60. L. M. Duan, E. Demler, and M. D. Lukin, Controlling spin exchange interactions of ultracold atoms in optical lattices, *Phys. Rev. Lett.* 91(9), 090402 (2003)
61. S. Trotzky, P. Cheinet, S. Fölling, M. Feld, U. Schnorrberger, A. M. Rey, A. Polkovnikov, E. A. Demler, M. D. Lukin, and I. Bloch, Time-resolved observation and control of super-exchange interactions with ultracold atoms in optical lattices, *Science* 319(5861), 295 (2008)

62. Y. Makhlin, G. Schön, and A. Shnirman, Quantum-state engineering with Josephson-junction devices, *Rev. Mod. Phys.* 73(2), 357 (2001)

63. J. Siewert and R. Fazio, Quantum algorithms for Josephson networks, *Phys. Rev. Lett.* 87(25), 257905 (2001)

64. D. V. Averin and C. Bruder, Variable electrostatic transformer: Controllable coupling of two charge qubits, *Phys. Rev. Lett.* 91(5), 057003 (2003)

65. C. Testelin, F. Bernardot, B. Eble, and M. Chamarro, Hole-spin dephasing time associated with hyperfine interaction in quantum dots, *Phys. Rev. B* 79(19), 195440 (2009)

66. Y. P. Shim, S. Oh, X. D. Hu, and M. Friesen, Controllable anisotropic exchange coupling between spin qubits in quantum dots, *Phys. Rev. Lett.* 106(18), 180503 (2011)

67. B. Urbaszek, X. Marie, T. Amand, O. Krebs, P. Voisin, P. Maletinsky, A. Högele, and A. Imamoglu, Nuclear spin physics in quantum dots: An optical investigation, *Rev. Mod. Phys.* 85(1), 79 (2013)

68. L. Viola, S. Lloyd, and E. Knill, Universal control of decoupled quantum systems, *Phys. Rev. Lett.* 83(23), 4888 (1999)

69. G. F. Xu, D. M. Tong, and E. Sjöqvist, Path-shortening realizations of nonadiabatic holonomic gates, *Phys. Rev. A* 98(5), 052315 (2018)

70. P. Z. Zhao, X. Wu, and D. M. Tong, Dynamical-decoupling protected nonadiabatic holonomic quantum computation, *Phys. Rev. A* 103(1), 012205 (2021)